EurJIC European Journal of Inorganic Chemistry

ChemPubSoc Europe

FULL PAPER

DOI:10.1002/ejic.201201126

Dinuclear Complexes with a Triple *N*1,*N*2-Triazole Bridge That Exhibit Partial Spin Crossover and Weak Antiferromagnetic Interactions

CLUSTER ISSUE

Olivier Roubeau,*[a] Patrick Gamez,*[b,c] and Simon J. Teat[d]

Keywords: Triazole / Coordination compounds / Iron / Spin crossover / Magnetic properties

The reaction of 4-phenylimino-1,2,4-triazole (**1**) with Fe^{II}, Co^{II}, Ni^{II} and Cu^{II} thiocyanate produces a series of analogous dinuclear compounds of formula $[M_2(\mathbf{1})_5(NCS)_4]$ (**2**–**5**) as demonstrated by single-crystal X-ray diffraction studies of the Fe^{II} (**2**) and Co^{II} (**3**) analogues. The magnetic properties of $[Fe_2(\mathbf{1})_5(NCS)_4]\cdot x$MeOH ($x$ = 3.5–5) reveal a partial and gradual spin crossover (SCO) centred at T_{SCO} = 115 K. This is confirmed by its crystal structure solved at 100, 150 and 250 K, which exhibits a gradual decrease of the Fe–N bond lengths with temperature. However, the bulk hydrated form of **2** that is generated upon exposure to air of crystals is a high-spin compound that exhibits weak antiferromagnetic interaction. The exchange coupling among the Fe^{II} $S = 2$ ions within the dinuclear neutral complex was evaluated as J/k_B = –1.33(3) K by using the Heisenberg Hamiltonian $H = -2JS_1\cdot S_2$. Similarly, the magnetic properties of the Ni^{II} (**4**) and Cu^{II} (**5**) analogues are dominated by moderate and weak antiferromagnetic interactions evaluated as J/k_B = –13.9(3) and –0.30(5) K, respectively. The presence of strong spin–orbit coupling of the individual Co^{II} ions impeded the evaluation of the likely antiferromagnetic interaction that leads to a singlet ground state in **3**. The reported structures of **2** and **3** are new additions to a very scarce family of dinuclear complexes bearing a unique triple *N*1,*N*2-triazole bridge. Owing to its relevance in the peculiar properties of 1D triazole-based SCO materials, which are widely studied for their various potential applications, a structural analysis of this triple *N*1,*N*2-triazole bridge in reported structures of Fe^{II} and Co^{II} trinuclear and 1D compounds is provided.

Introduction

The spin-crossover (SCO) phenomenon is often depicted as the paradigm of bistability at the molecular level.[1] This is especially true for Fe^{II} compounds for which the low-spin (LS) to high-spin (HS) transitions are associated with diamagnetic to paramagnetic switching together with significant optical and Fe–L bond-length changes.[2] These changes can be triggered not only by temperature changes, but also through other external stimuli, such as irradiation or pressure.[3] For an Fe^{II} ion to have the adequate ligand-field strength for the occurrence of SCO, triazole and tetrazole ligands are known to be ideal donors.[4] In the case of triazole, a bridging *N*1,*N*2 coordination mode is usually observed, as exemplified by the vast family of polymeric one-dimensional triazole-based Fe^{II} materials[5] of general formula $[Fe(Rtrz)_3](A)_2\cdot xH_2O$ (Rtrz = 4-substituted-1,2,4-triazole), in which the Fe^{II} ions are linked through three *N*1,*N*2-triazole bridges. These classic SCO compounds have been at the centre of many recent developments towards applications[6] and have allowed the design of early optical-device prototypes,[7] the elaboration of SCO nanoparticles,[8] supramolecular gels,[9] thin films,[10] dendrimers,[11] contrast agents for magnetic resonance imaging[12] and liquid crystals,[13] as well as the electrical addressing of SCO[14] or the use of plasmons to detect SCO.[15] One of the key advantages of these materials is their chemical flexibility, while maintaining the coordination chains of Fe^{II} connected by triple *N*1,*N*2-triazole bridges. This short, rigid – though strainless and thus very stable linkage (see Scheme 1, left) – is what really makes the triazole 1D systems unique. On one hand, it represents an effective propagation medium for the variation of coordination sphere volume upon SCO, as opposed to flexible linkers. On the other hand, its stability combined with the possibility to modify the triazole ring at the 4-position gives access to families of compounds, as indeed has been the case with the 1D

[a] Instituto de Ciencia de Materiales de Aragón (ICMA), CSIC and Universidad de Zaragoza,
Plaza San Francisco, 50009 Zaragoza, Spain
Fax: +34-976-761229
E-mail: roubeau@unizar.es
Homepage: http://fmc.unizar.es/people/roubeau
[b] Departament de Química Inorgànica, QBI, Universitat de Barcelona,
Martí I Franquès 1–11, 08028, Barcelona, Spain
Fax: +34-934-907725
E-mail: patrick.gamez@qi.ub.es
Homepage: http://www.bio-inorganic-chemistry-icrea-ub.com
[c] Institució Catalana de Recerca i Estudis Avançats (ICREA), Passeig Lluís Companys 23, 08010 Barcelona, Spain
[d] Advanced Light Source, Lawrence Berkeley National Laboratory,
1 Cyclotron Road, Berkeley, CA 94720, USA

Supporting information for this article is available on the WWW under http://dx.doi.org/10.1002/ejic.201201126.

$[Fe(Rtrz)_3](A)_2$ system, the SCO temperature and cooperative character of which can be tuned by the nature of the 4-substituent on the triazole ligand and/or the choice of the counteranion.[5a,5b] The drawback of these materials is their usually poor crystallinity, which is probably due to their polymeric nature. Indeed, the first crystal structure of an $[Fe(Rtrz)_3](A)_2$ compound has only very recently been reported.[16] Previously, structurally characterized Cu^{II} analogues[17] or trinuclear compounds with an $[Fe(Rtrz)_3$-$Fe(Rtz)_3]$ core[18] were used as structural models and for comparison in extended X-ray absorption fine structure (EXAFS) studies of the Fe^{II} chain compounds.[19] Surprisingly, the simpler dinuclear compounds with one central triple *N*1,*N*2-triazole bridge are extremely scarce in the literature, and most of them involve thiocyanate ions as terminal ligands.[20] Specifically with Fe^{II}, the recently reported SCO compound $[Fe_2(N$-salicyliden-4-amino-1,2,4-triazole$)_5$-$(NCS)_4]\cdot 4MeOH$ and the peculiar dimer–monomer compound $[Fe_2(4$-*p*-tolyl-1,2,4-triazole$)_5(NCS)_4][Fe(4$-*p*-tolyl-1,2,4-triazole$)_2(NCS)_2(H_2O)_2]$ are the only other known structures with a unique triple *N*1,*N*2 bridge.[20e,20f] We report here on two additions to this short list, obtained with the 4-phenylimino-1,2,4-triazole (**1**) ligand, namely, $[Fe_2(\mathbf{1})_5$-$(NCS)_4]\cdot x$MeOH (**2**·xMeOH; x = 0, 3.5, 5) and $[Co_2(\mathbf{1})_5$-$(NCS)_4]\cdot 3.5$MeOH (**3**·3.5MeOH). We also report the Ni^{II} (**4**) and Cu^{II} (**5**) analogues, although their structures could not be obtained so far. Variable-temperature X-ray diffraction and magnetic measurements reveal that the solvated Fe^{II} compound exhibits a partial SCO and that all compounds present weak antiferromagnetic interactions. A structural comparison of the triple *N*1,*N*2-triazole bridges in these dinuclear compounds with those in reported structures of trinuclear and 1D Fe^{II}[18] and Co^{II}[21] compounds has been made.

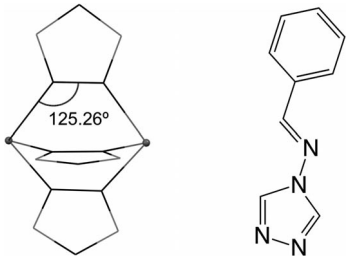

Scheme 1. Left, idealized geometry of triple *N*1,*N*2-1,2,4-triazole coordination bridge of two metal ions (small grey spheres) to give M–N–N angles close to the exocyclic free donor electron pair angle of a regular five-membered ring (126°). N and C atoms are in black and light grey respectively. Right, 4-phenylimino-1,2,4-triazole ligand **1**.

Results and Discussion

Synthesis

Triazole ligands substituted solely at their 4-position are usually able to coordinate in the desired *N*1,*N*2-bridging mode. Arylimino-substituted 4-amino-1,2,4-triazoles, easily obtained in high yields, have been prepared with the objective of generating π–π stacking interactions that may help to create intermolecular contacts, and therefore potentially favour more cooperative SCO behaviours. Thus, the phenyl, naphthyl and anthracyl derivatives have been synthesized. However, to date, only coordination complexes with the phenyl-containing ligand could be isolated. 4-Phenylimino-1,2,4-triazole (**1**, Scheme 1, right) is obtained readily from the reaction of 4-amino-1,2,4-triazole and benzaldehyde in ethanol. The coordination compounds **2**–**5** were synthesized by the direct addition of a methanolic solution of the phenyliminotriazole ligand **1** to a freshly prepared methanolic solution of $M(NCS)_2$ (M = Fe, Co, Ni, Cu), obtained from M^{II} sulfate and ammonium thiocyanate (see Experimental Section). In the case of **2**, the synthesis was performed under argon to prevent oxidation of Fe^{II} to Fe^{III}. Although rather dilute solutions were used, the precipitation of **2**–**5** as crystalline powders occurred within 24 h. More of the crystalline material was obtained by slow concentration of the remaining solution after recovering the bulk powder by filtration, including single crystals of **2** and **3** suitable for X-ray diffraction studies. The latter were thus found to form as methanolates of the dinuclear $[M_2(\mathbf{1})_5(NCS)_4]$ species (M = Fe, Co; see below). If more concentrated conditions or more than 2.5 equiv. of **1** per M^{II} ion are used, an unidentified solid, probably formed of linear coordination oligomer/polymers, precipitates rapidly. As previously observed in some of the other reported similar compounds,[20b,20f] the crystals disaggregate when exposed to air, which indicates that the lattice solvent molecules probably play an important role in stabilizing these structures. However, the IR spectra of crystals maintained in a small amount of MeOH, the dry powdered crystals and the bulk powders are all very similar (see Experimental Section), which indicates that they all consist of the same dinuclear complex. In particular, the observation of two out-of-plane ring torsion bands (at ca. 620 and 680 cm^{-1}) indicate the presence of both mono- and bidentate triazole ligands.[22] Moreover, the ν(CN) band of the NCS^- ion is in the range 2000–2150 cm^{-1}, which indicates coordination through its N donor atom, and only presents a shift ascribable to the difference in M–N bond length. Elemental analyses of the powder samples are in agreement with hydrates of the $[M_2(\mathbf{1})_5(NCS)_4]$ complexes, which result from the absorption of moisture from air.

Description of Crystal Structures

The molecular structure of **2** was determined at 100 and 250 K on a first crystal and at 150 K on a second crystal. At these temperatures, lattice solvent loss is (partially) prevented, and **2** crystallizes in the triclinic space group $P\bar{1}$. The asymmetric unit contains one full neutral dinuclear complex plus five lattice methanol molecules, although in the first crystal some of these are partially occupied resulting in a total of 3.5 methanol molecules. The two Fe sites in the dinuclear units are bridged by three *N*1,*N*2-tri-

azole rings of **1** and separated by 3.789/3.953/3.967 Å, respectively, at 100/150/250 K. Their coordination spheres are each completed by one terminal triazole *N*1-donor and two *cis*-thiocyanates. An ORTEP view of the dinuclear unit at 100 K is shown in Figure 1. The terminal C–S bond of one of the thiocyanate ions coordinated to Fe1 is disordered over two positions, and the component corresponding to the eclipsed position (see Figure 2) has a relative occupancy of 0.61/0.58/0.48. The environment and bond lengths of the two Fe sites are very similar at the three temperatures (see Table 1). The average Fe–N bond lengths at 250 K are typical of an Fe^{II} ion in its HS state, whereas the lower values at 150 and 100 K clearly indicate the process of SCO. This also agrees with the purple colour of the crystal at 100 K, whereas it is yellow at ambient temperature, and is the origin of the shorter intramolecular Fe···Fe separation at 100 K. Nevertheless, the Fe–N bonds at 100 K are still longer than those expected for a fully LS state with this environment. In fact, considering the LS and HS structures of the only other related SCO dinuclear compound as a reference,[20f] the Fe1 and Fe2 sites would be 55 and 58% LS Fe^{II}, respectively. This is in good agreement with the magnetic measurements (see below), and points at a continuous and concomitant SCO at both Fe sites, without any sign of HS–LS pairs. The FeN_6 polyhedron remains close to an octahedron at all temperatures for both Fe sites (see Figure 2 and Tables 1, S2 and S3) and has only a rather small distortion, which is smaller at the lowest temperature, as expected for an LS state. The triazole rings are fairly planar with their planes parallel to the molecular axis. At 100 K, their centroids form mutual angles of 114, 115.7 and 130.3° with respect to the Fe···Fe axis midpoint, and the average value is close to 120° as in a tri-wing paddlewheel (see Figure 2). The Fe–N–N angles range from 122.9 to 128.4°, all close to 126°, which corresponds to the exocyclic free electron pair angle of a regular five-membered ring. The average values are 125.53, 125.9 and 126.0° at 100, 150 and 250 K, respectively. This clearly results in no significant

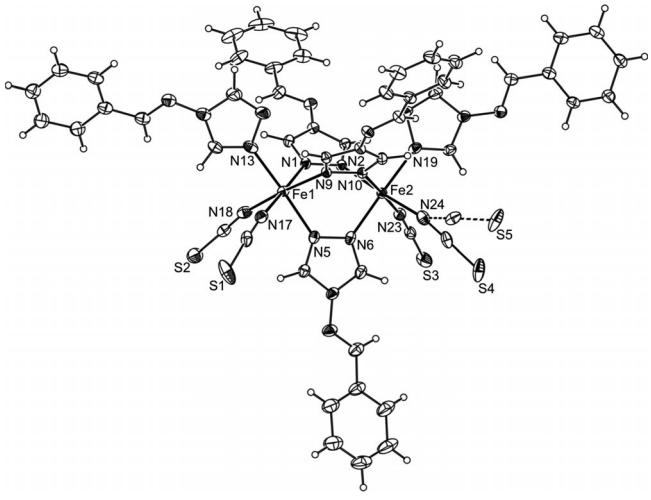

Figure 1. ORTEP view of the dinuclear complex in **2**·3.5MeOH at 100 K; ellipsoids at 30% probability. Only the metal, sulfur and nitrogen atoms involved in coordination bonds are labelled.

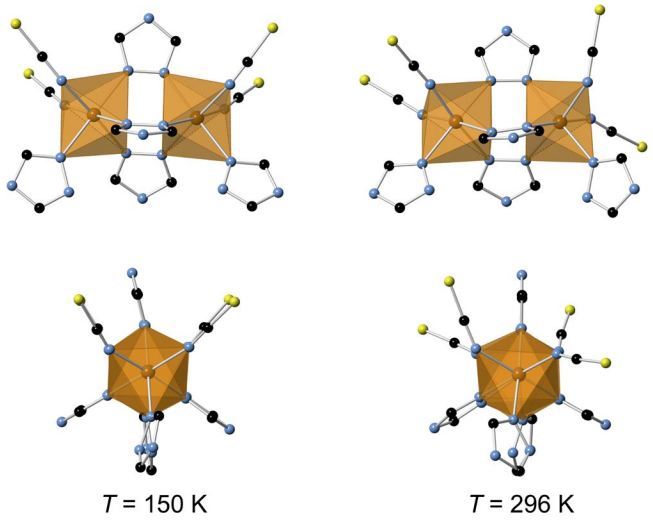

Figure 2. Views of the structures of **2**·5$H_2$0 at 150 K (left) and **2** at 296 K (right) perpendicular (top) and along (bottom) the Fe···Fe axis, which show the different orientation adopted by the thiocyanate ions; the FeN_6 coordination spheres are highlighted as brown polyhedra. The phenylimino groups are not shown for clarity. Colour code: Fe brown, S yellow, N light blue, C black.

Table 1. Structural parameters describing the coordination environment of the metal sites in the dinuclear complexes of **2**·3.5MeOH (100 and 250 K), **2**·5MeOH (150 K), **2** (296 K) and **3**·3.5MeOH (100 K).

	2				**3**
T	100 K	150 K	250 K	296 K	100 K
M1–N1	2.064(2)	2.189(6)	2.195(2)	2.184(11)	2.129(2)
M1–N5	2.080(2)	2.188(6)	2.201(3)	2.180(11)	2.154(2)
M1–N9	2.088(2)	2.211(6)	2.214(2)	2.214(12)	2.162(2)
M1–N13	2.070(3)	2.173(7)	2.175(3)	2.170(12)	2.128(2)
M1–N17	2.012(3)	2.107(8)	2.099(3)	2.064(19)	2.081(2)
M1–N18	2.034(3)	2.125(7)	2.134(3)	2.160(13)	2.102(2)
Σ[a]	20.21	23.30	22.83	23.80	24.60
$M1–N_{NCS}$[b]	2.023	2.116	2.116	2.112	2.091
$M1–N_{trz}$[b]	2.075	2.190	2.196	2.187	2.143
M1–N[b]	2.058	2.166	2.170	2.162	2.126
%HS[c]	0.55	0.02	–	–	–
M2–N2	2.055(2)	2.178(6)	2.184(2)	2.221(11)	2.123(2)
M2–N6	2.053(3)	2.186(7)	2.193(3)	2.198(13)	2.137(2)
M2–N10	2.056(2)	2.174(6)	2.190(3)	2.251(13)	2.129(2)
M2–N19	2.073(3)	2.178(7)	2.192(3)	2.148(14)	2.147(2)
M2–N23	2.012(3)	2.081(8)	2.093(3)	2.120(16)	2.081(3)
M2–N24	2.031(3)	2.143(7)	2.138(3)	2.162(15)	2.109(3)
Σ[a]	16.96	27.40	22.91	27.70	19.31
$M2–N_{NCS}$[b]	2.021	2.112	2.115	2.141	2.095
$M2–N_{trz}$[b]	2.059	2.179	2.190	2.204	2.134
M2–N[b]	2.047	2.157	2.165	2.183	2.121
%LS[c]	0.58	0.04	–	–	–

[a] Distortion of the FeN_6 polyhedron from octahedral, $\Sigma = \Sigma(\theta - 90)$, θ is the N–Fe–N angle between vertex-sharing pairs of N donors.[24] [b] Averaged values. [c] Derived from the decrease in average Fe–N bond length with respect to the fully HS case (taken from the structure at 250 K) and compared to the decrease observed in $[Fe_2(N\text{-salicyliden-4-amino-1,2,4-triazole})_5(NCS)_4]$·4MeOH, which corresponds to a full HS–LS transition.[20f]

strain and compares well with observed values in other dinuclear, trinuclear and 1D structures built on such triple *N*1,*N*2-triazole bridges (see below).

The neutral dinuclear units form a dense 3D network through intermolecular interactions of various types. Tables S4 and S5 gather the details of all intermolecular interactions in the structures described in the present report. In **2**·3.5MeOH at 100 K two of the bridging **1** ligands strongly interact with one counterpart of two neighbouring dimers through parallel double π–π stacking interactions of their respective phenyl and iminotriazole groups (red lines in Figure S2, Table S4). The resulting supramolecular zigzag chain of dimers remains similar at 150 and 250 K. The third bridging **1** ligand interacts in a similar manner with the monocoordinated **1** to Fe2 of another neighbouring complex; however, in this case, the two phenyliminotriazole rings are rotated with respect to each other resulting in only one single π–π stack (green line in Figure S2, Table S4). This latter weaker π-stacking contact is not observed at higher temperatures. The sulfur atoms of the two thiocyanates coordinated to Fe2 form S···H–C interactions with the phenyl and triazole rings of three different neighbouring [Fe_2] complexes, as well as an S···π contact with a terminal triazole ring (Figure S3, Table S4). The thiocyanate sulfur atoms also act as H-bond acceptors for the hydroxy hydrogen atoms of the lattice MeOH molecules (Figure S4, Table S4). The MeOH oxygen atoms in turn are acceptors in strong H-bonds with triazole and imine hydrogen atoms. However, these H-bonds do not participate in intercomplex interactions.

Warming the second crystal to 296 K resulted in poorer diffraction; however, the data collected were of sufficient quality and showed that the crystal had lost its lattice methanol molecules. Because the crystal was kept in a dry flow of N_2, no air moisture was absorbed. Attempts to measure crystals exposed to air failed owing to powdering. At 296 K, desolvated **2** still crystallizes in the triclinic $P\bar{1}$ space group in a similar cell, but with the *a* and *b* axes and corresponding angles *α* and *β* inter-exchanged. The asymmetric unit now only contains the dinuclear neutral complex, which is comparable in most aspects to that of the solvated structures (Tables 1, S2 and S3), although no disorder of any thiocyanato ligand is observed. An important difference is found in the orientation of the thiocyanato ligands (Table S3); whereas they are almost perfectly eclipsed when looking along the Fe1···Fe2 axis in the lower temperature structures, which have S1–N17–N24–S4/S2–N18–N23–S3 torsion angles of 1.78/–3.68° at 150 K, their orientation strongly differs at 296 K, with torsion angles of 84.57/43.08° (see Figure 2). This probably has an effect on the ligand field exerted by the thiocyanato ligands. However, the structure of **2** maintains the zigzag chains of dinuclear complexes formed through π-stacking interactions of two of the bridging **1** ligands with similar geometries as that observed in the solvated structures (Table S5). Additional S···H–C interactions involving three of the thiocyanate sulfur atoms (Figure S5 and Table S5) result in a rather intricate network of supramolecular interactions.

At 100 K, **3** is isomorphous to **2** and crystallizes in the triclinic $P\bar{1}$ space group with a neutral dinuclear complex [Co_2(**1**)$_5$(NCS)$_4$] and a total of 3.5 methanol molecules forming the asymmetric unit. All structural parameters of the dinuclear complex, including the disorder shown by one of the thiocyanate ions and their eclipsed orientation, and the intermolecular interactions are very similar to those of **2**·3.5MeOH at 100 K (see Figure S6, Tables 1, S4, S5 and S6). This supports the proposal to use Co^{II} compounds as structural (HS) references for spin-crossover Fe^{II} analogues.[23]

Magnetic Properties

The temperature dependence of χT (χ is the molar paramagnetic susceptibility) of compounds **2**–**5** as bulk crystalline powders were derived from magnetization measurements in an applied field of 0.5 T (0.1 T for **3**) and in the temperature range 2–300 K. Data were also obtained for fresh crystals of **2**·5MeOH kept in a small amount of MeOH to avoid modifications of the magnetic properties upon possible solvent loss. The data for **2**·5MeOH and dry **2**, shown in Figures 3 and 4, respectively, corroborate the structural observations and evidence the occurrence of a partial thermal SCO for intact crystals of **2**·5MeOH and the absence of such a process for dry **2**. Indeed, χT of **2**·5MeOH decreases upon cooling from 6.81–6.70 $cm^3 mol^{-1} K$ in the range 250–170 K, in agreement with two Fe^{II} ions in their HS $S = 2$ state (6 $cm^3 mol^{-1} K$ for $g = 2$), and reaches a plateau at ca. 3.35 $cm^3 mol^{-1} K$ at 60–50 K. Further decrease then sets in down to 0.50 $cm^3 mol^{-1} K$ at 2 K. Compound **2**·5MeOH thus undergoes a partial and gradual SCO centred at ca. 115 K. In reasonable agreement with the structural observations at 100 K, the plateau reached at ca. 60 K has a χT value corresponding to ca. 50% of the Fe^{II} ions in their LS state. The further lowering of χT below 50 K is probably caused by a combination of zero field splitting (ZFS) effects of the remaining $S = 2$ ions and antiferromagnetic interactions within the corresponding dinuclear complexes (see below). These observations are reproducible upon warming over various cycles and over several batches of crystals as long as the sample is kept in contact with MeOH and the temperature is not brought above 250 K. On the other hand, χT for the bulk powder of **2** (most likely its hydrated form, see Experimental Section) remains practically constant at 6.9–6.6 $cm^3 mol^{-1} K$ (again in agreement with the presence of two Fe^{II} ions in their HS state) from 300 K down to 60 K; below this temperature, χT starts to decrease more and more abruptly to reach a value of 1.06 $cm^3 mol^{-1} K$ at 1.8 K. The magnetic properties of **2** are thus in agreement with an $S = 2$ HS ground state for the Fe^{II} ion with *g* close to 2 throughout the whole temperature range considered; the decrease at low temperatures is due to a combination of ZFS of the $S = 2$ spins and weak antiferromagnetic interaction. An evaluation of the antiferromagnetic interaction through the triple *N*1,*N*2-triazole bridge can be obtained by neglecting the ZFS, which

for octahedral HS Fe^{II} centres should be rather small. Thus, the analytical expression of the magnetic susceptibility derived[25] by applying the van Vleck equation and Kambé vector coupling method to the Heisenberg Hamiltonian $H = -2JS_1 \cdot S_2$ in the mean-field approximation was used to fit the experimental data. The resulting best fit (full line in Figure 4) was obtained for $g = 2.18(2)$ and $J/k_B = -1.33(3)$ K.

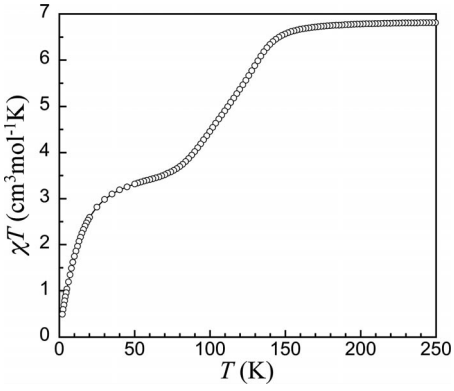

Figure 3. χT vs. T plot for crystals of **2**·5MeOH kept in contact with a small amount of MeOH.

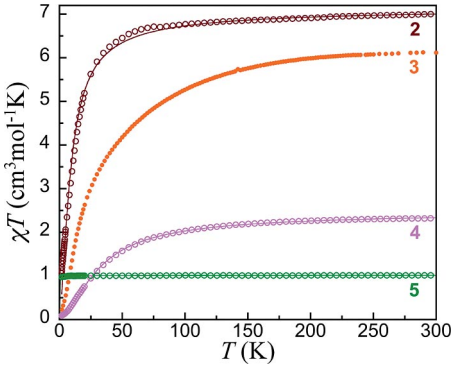

Figure 4. χT vs. T plots for **2**–**5**. Full lines are fits to the analytical Heisenberg expression for the susceptibility of pairs of coupled $S = 2$ (**2**), 1 (**4**) and 1/2 (**5**) spins (see text).

Similarly to that for **2**, the χT vs. T data for **3**, **4** and **5** (Figure 4) show a plateau at higher temperatures (above 200, 150 and 10 K, respectively) in agreement with two $S = 3/2$ Co^{II}, $S = 1$ Ni^{II} and $S = 1/2$ Cu^{II} spins at 6.1–6.0, 2.3–2.2 and 1.01–1.005 $cm^3 mol^{-1} K$, respectively. At lower temperatures, a decrease sets in down to 0.11, 0.09 and 0.97 $cm^3 mol^{-1} K$, respectively, at 2 K. For **3**, this decrease already occurs from 200 K and probably involves both intramolecular antiferromagnetic interactions that leads to a singlet ground state and intrinsic strong spin–orbit coupling of the HS Co^{II} ions, which results in the stabilization of a doublet ground state, for each individual Co^{II} ion in the dimer.[26] This makes the analysis of the magnetic properties difficult and impeded the modelization of the experimental data for **3**. For **4**, an evaluation of the antiferromagnetic interaction can be obtained by neglecting the ZFS of the Ni^{II} ions. This is reasonable as it will likely be active only at low temperatures, whereas χT already decreases significantly at 150 K. Thus, the experimental data were fitted to the corresponding Heisenberg expression for the magnetic susceptibility and yielded the best parameters $g = 2.25(1)$ and $J = -13.9(2)$ K (full line in Figure 4). This moderate antiferromagnetic exchange coupling should be taken as an upper limit to the actual interaction propagated by the *N*1,*N*2-triazole bridge in **4**. For **5**, the decrease at low temperatures can only be due to antiferromagnetic interactions, and the experimental data are properly reproduced by the analytical Heisenberg expression for the magnetic susceptibility. The best fit is obtained for $g = 2.32(1)$ and $J/k_B = -0.30(5)$ K (full line in Figure 4), and thus confirms that only a very weak antiferromagnetic interaction is present in **5**.

The Triple *N*1,*N*2-Triazole Bridge – a Rigid Constraint

The structural parameters that describe transition metal ion pairs bridged by three *N*1,*N*2–1,2,4-triazole ligands reported in the literature for Fe^{II} and Co^{II} are gathered in Table 2. These include only dinuclear and trinuclear compounds and one coordination polymeric chain compound. It appears that the topology of the triple *N*1,*N*2-1,2,4-triazole bridges remains very similar in these compounds and is very close to the idealized geometry shown in Scheme 1. This is clearly evidenced by the M–N–N angles, for which not only the average values for the three triazoles and the two metal ions remain very close to the ideal value of 125.26°, but also every single angle does not depart more than 5° from it. The mutual dihedral angles of the triazole rings are already close to 120° in most compounds, and the average values are actually virtually equal to 120°. In fact, deviations from this value for certain pairs of triazole rings are all related to the presence of either external intermolecular interactions, for example, the strong π–π stacking interactions in **2**·3.5MeOH and **3**·3.5MeOH or the H-bonding between dinuclear and mononuclear moieties in $[Fe_2(ptoltrz)_5(NCS)_4]\cdot[Fe(ptoltrz)_2(H_2O)_2(NCS)_2]$,[20d] or disorder as in $[Fe_2(salatrz)_5(NCS)_4]\cdot 4MeOH$.[20f] This structural stability of the M–(*N*1,*N*2-trz)$_3$–M bridge happens even though the other "side" of each metal atom of the bridged pair actually differs significantly; the three *fac* coordination sites may indeed be occupied by either solvent molecules, terminal neutral ligands, including monocoordinated triazoles, anions, or another triple triazole bridge. The only dissymmetric dinuclear complex of this family of compounds, $[Co_2(altrz)_4(H_2O)(NCS)_4]\cdot 2H_2O$, is in this respect exemplar;[20c] although the coordination environment of the two Fe sites are completed by either an 4-allyl-1,2,4-triazole ligand or a water molecule, very similar triazole M–N bond lengths and M–N–N angles are observed for both metal sites. Similarly, in trinuclear compounds obtained with *p*-MeOprtrz[18c] the external Fe^{II} sites have a much more distorted octahedral environment, but this has only a slight effect on the characteristics of their triple *N*1,*N*2-1,2,4-triazole bridges.

Table 2. Structural parameters describing the M–(*N*1,*N*2-trz)$_3$–M moiety in all reported Fe^{II} and Co^{II} coordination compounds containing one triple *N*1,*N*2-triazole bridge.[a]

Compound[b]	*T* [K]	M···M [Å]	M–N[c][d] [Å]	Σ	N–N–M[c] [°]	trz–trz angles[e] [°]	T_{SCO} [K]	Ref.
2·3.5MeOH	100	3.789	2.077/2.055	20/17	125.6	119.9 (109.4–136.8)	115	[f]
	250	3.967	2.203/2.189	23/23	126.0	119.9 (109.1–136.9)		
2	296	3.995	2.193/2.223	24/28	126.1	119.7 (117.8–122.4)	HS	[f]
3·3.5MeOH	100	3.903	2.147/2.130	25/19	126.0	120.0 (108.7–138.2)	–	[f]
$[Co_2(Phtrz)_5(NCS)_4]\cdot 2.7H_2O$	r.t.	3.907	2.142/2.157	18/25	125.8	119.5 (114.3–126.1)	–	[20b]
$[Co_2(altrz)_4(H_2O)(NCS)_4]\cdot 2H_2O$	r.t.	3.909	2.147/2.142	21/11	124.9/126.8	119.8 (118.5–121.0)	–	[20c]
$[Fe_2(ptoltrz)_5(NCS)_4]\cdot[Fe(ptoltrz)_2(H_2O)_2(NCS)_2]$	r.t.	3.937	2.192/2.189	23/26	125.5	119.7 (106.4–133.9)	111	[20d]
$[Co_2(atrz)_3(H_2O)_4(tp)_2]\cdot 11H_2O$	130	3.823	2.114	21	125.1	119.7 (115.6–127.9)	–	[20e]
$[Fe_2(salatrz)_5(NCS)_4]\cdot 4MeOH$	100	3.648	1.962	19	125.1	120.0 (116.6–122.1)	150	[20f]
	200	3.966	2.165	15	125.9	119.6 (117.0–122.1)		
$[Fe_3(etrz)_6(H_2O)_6](CF_3SO_3)_6$	105	3.795	2.031/2.176	28/32	126.1/123.6	119.9	205	[18b]
	300	3.840	2.174/2.157	10/25	124.5/124.3	119.7		
$[Fe_3(p\text{-}MeOptrz)_8(H_2O)_4](BF_4)_6\cdot 2H_2O$	r.t.	3.868	2.175/2.146	15/30	123.8/125.8	120.0 (114.3–129.9)	HS	[18c]
$[Fe_3(p\text{-}MeOptrz)_6(H_2O)_6](tos)_6\cdot 2MeOH\cdot 8H_2O$	r.t.	3.793	2.177/2.124	5/35	125.4/122.1	119.3 (113.9–126.2)	330	[18c]
$[Fe_3(iprtrz)_6(H_2O)_6](tos)_6\cdot 2H_2O$	r.t.	3.833[c]	2.167/2.159	11/22	124.7/124.5	120.0 (112.4–125.4)	242	[18d]
$[Fe_3(hyetrz)_6(H_2O)_6](CF_3SO_3)_6$	120	3.783	2.003/2.161	20/20	125.7/122.7	120.0	290	[18e]
	330	3.832	2.169/2.176	9/21	127.6/122.7	120.0		
$[Fe_3(prtrz)_6(H_2O)_6](ReO_4)_6\cdot H_2O$	r.t.	3.862	2.191/2.157	21/21	123.6/124.6	119.8	185	[18f]
$[Fe_3(npt)_6(EtOH)_4(H_2O)_2](tos)_2\cdot 4EtOH$	100	3.839	2.151/2.163	17/27	127.0/125.3	119.7 (115.9–121.7)	148	[18g]
	181	3.867	2.009/2.145	9/19	125.5/124.6	119.7 (116.0–121.7)		
$[Co_3(npt)_6(EtOH)_4(H_2O)_2](tos)_2\cdot 4EtOH$	202	3.863	2.141/2.127	7/15	125.1/125.6	119.8 (116.1–121.7)	–	[18g]
$[Co_3(npt)_6(MeOH)_4(H_2O)_2](tos)_2\cdot 4EtOH$	202	3.853	2.137/2.105	14/20	126.1/124.7	119.3 (116.0–127.2)	–	[18g]
$[Fe(atrz)_3](NO_3)_2\cdot 2H_2O$	120	3.655	1.95/1.99	15/11	123.9/127.2	119.9 (117.6–122.7)	[g]	[16]

[a] The structure of $[Co_3(metrz)_6(H_2O)_6][Co_3(metrz)_8(H_2O)_4](CF_3SO_3)_{12}\cdot 8H_2O$ (metrz = 4-methyl-1,2,4-triazole) is not included owing to its poor quality.[18h] Note that $[Co^{II}_2Co^{III}(HL)^2(L)_4(H_2O)_6]Cl_3\cdot 9H_2O$ (HL = 3,5-diamino-1,2,4-triazole) is not included in this summary due to its mixed-valent character and the presence of charged triazolate.[21b] [b] Phtrz = 4-phenyl-1,2,4-triazole; altrz = 4-allyl-1,2,4-triazole; ptoltrz = 4-(*p*-tolyl)-1,2,4-triazole; atrz = 4-amino-1,2,4-triazole; tp = terephthalate; salatrz = *N*-salicyliden-4-amino-1,2,4-triazole; etrz = 4-ethyl-1,2,4-triazole; *p*-MeOptrz = 4-(*p*-methoxyphenyl)-1,2,4-triazole; iprtrz = 4-isopropyl-1,2,4-triazole; tos = *p*-toluenesulfonate; hyetrz = 4-(2′-hydroxyethyl)-1,2,4-triazole; prtrz = 4-propyl-1,2,4-triazole; npt = 4-(4′-nitrophenyl)-1,2,4-triazole. [c] If there are various values (depending on symmetry), then the average value is given. In the case of M–N bond lengths, only those corresponding to triazole rings participating in the triple *N*1,*N*2-bridge are averaged. [d] Values are given for each M crystallographic site. For trimers, the first value corresponds to the central metal ion that exhibits SCO for M = Fe, and the second to the outer metal ion. [e] Mutual dihedral angles between the planar triazole rings. The first value is the average or unique value. Values in parentheses are the maximum and minimum angles. [f] This work. [g] The structure indicates an LS state at 120 K. The dehydrated sample has an abrupt SCO with a large hysteresis above r.t.[5b]

It is therefore evident that the geometry of the triple *N*1,*N*2-triazole bridge is maintained with only very small variations whatever the environment of the M–(*N*1,*N*2-trz)$_3$–M moiety and is a dominant parameter in the structures in which it is involved. Through its stability, the M–(*N*1,*N*2-trz)$_3$–M bridge thus acts as a constraint on the rest of the metal coordination sphere towards a regular octahedral geometry. This is well shown by the small distortion parameters Σ observed for all Fe^{II} and Co^{II} ions in this family of compounds (Table 2). Such a constraint would clearly become stronger in longer systems, and this is probably what makes the 1D coordination polymers of formula $[Fe(Rtrz)_3](A)_2$ peculiar; the repetition of triple bridges forces the Fe^{II} ions into a rigid and regular octahedron. Then, the structural modifications induced by the coordination sphere volume variation upon the SCO will thus mostly be propagated along the M···M axis, so that the stable geometry of the M–(*N*1,*N*2-trz)$_3$–M moiety is maintained. Clearly, with a variation of the coordination sphere volume of up to 20% upon SCO,[20] such a rigidity represents a strong source of intrinsic cooperativity. However, this will only occur within extended linear structures, in which the SCO will result in a strong elongation (or compression) of the coordination chains.[27] Nevertheless, additional interchain interactions are required to explain the very strong cooperativity of $[Fe(Htrz)_2(trz)](BF_4)$, for example.[28]

Eventually, the structurally constraining character of the M–(*N*1,*N*2-trz)$_3$–M bridge probably has synthetic consequences. Indeed, given the stability of the bridge, it is surprising that besides the coordination polymers, no longer oligomers than dinuclear and trinuclear complexes could be isolated so far. These are believed to coexist in solution,[4a] possibly in the presence of larger oligomers, and this is reasonable considering the corresponding syntheses involve very similar M/triazole ratios, typically from 1:2 to 1:2.5 for dimers and trimers, and 1:3 to 1:4 for 1D compounds. Possibly, the constrained structure created by repeating M–(*N*1,*N*2-trz)$_3$–M bridges is only stabilized by a certain number of repeating units, so that only longer oligomers are present in solution. These will only crystallize if a homogeneous length is reached, which could explain why only infinite coordination chains are crystallized. Shorter chains/oligomers have indeed only been reported from the breaking of preformed infinite chains, either at an air/water

interface during Langmuir–Blodgett deposition[10a] or from a heat-set gel–sol transition induced by the change of coordination number of Co^{II} ions.[29]

Conclusions

A series of dinuclear compounds of formula $[M_2(\mathbf{1})_5(NCS)_4]$ (M = Fe, Co, Ni, Cu) are obtained from the reaction of 4-phenylimino-1,2,4-triazole (**1**) with M^{II} thiocyanates. The crystals structures of the Fe^{II} and Co^{II} analogues are new additions to a very limited number of known structures containing one sole M–(*N*1,*N*2-trz)$_3$–M moiety. The structural parameters of this dinuclear unit as found in dinuclear, trinuclear and 1D structures in the literature are compared. The topology of the bridge is found to be maintained independently of its environment, which confirms its stability and highlights its rigidity and related constraints. The Fe^{II} analogue $[Fe_2(\mathbf{1})_5(NCS)_4]\cdot x$MeOH ($x$ = 3.5–5) is shown to present a gradual and incomplete spin crossover centred at 115 K as confirmed by both magnetic measurements and variable-temperature diffraction studies.

Experimental Section

Physical Measurements: FTIR spectra were recorded with pure solid samples with a Perkin–Elmer Spectrum 100 spectrometer equipped with a universal attenuated total reflectance (ATR) sampling accessory. Magnetic measurements were performed with an MPMS-XL superconducting quantum interference device (SQUID) magnetometer. Data were corrected for the experimentally determined sample holder diamagnetism and for the intrinsic diamagnetic susceptibility of the sample as calculated from Pascal tables.[30] Microanalyses were carried out with a Perkin–Elmer Series II CHNS/O Analyzer 2400 at the Servei de Microanalisi of CSIC (Barcelona, Spain). All reagents were commercially available and were used without purification. All manipulations were carried out under aerobic conditions, except where specified (compound **2**).

4-Phenylimino-1,2,4-triazole (1): 4-Amino-1,2,4-triazole was prepared from hydrazine monohydrate and formic acid. 4-Amino-1,2,4-triazole (7.23 g, 0.085 mol) was dissolved in absolute ethanol (14 mL). This solution was warmed to 50 °C, and benzaldehyde (11.7 g, 0.11 mol) dissolved in absolute ethanol (10 mL) was added. The resulting reaction mixture was heated to reflux for 5 h, and a white solid corresponding to crude **1** formed upon cooling. Recrystallization from EtOH/diethyl ether afforded a total (3 crops) of 12.7 g (0.073 mol) of pure **1**. Yield: 87%. ^{13}C NMR (300 MHz, acetone, 298 K): δ = 129.35, 129.95, 133.10 and 133.51 (phenyl), 158.26 (C=N) ppm. ^1H NMR (300 MHz, acetone, 298 K): δ = 7.58 (t, 3 H, phenyl), 7.93 (d, 2 H, phenyl), 8.91 (s, 2 H, triazole), 9.10 (s, 1 H, C=N) ppm. $C_9H_8N_4$ (172.19): calcd. C 62.78, H 4.68, N 32.54; found C 62.71, H 4.76, N 32.69. IR: $\tilde{\nu}$ = 3102, 3030, 3004, 2956, 1614, 1604, 1577, 1502, 1492, 1464, 1450, 1405, 1328, 1311, 1290, 1234, 1215, 1163, 1057, 941, 865, 750, 686, 621, 589, 503 cm^{-1}.

$[Fe_2(\mathbf{1})_5(NCS)_4]$ (2): $FeSO_4\cdot 7H_2O$ (278 mg, 1.00 mmol), NH_4NCS (157 mg, 2.06 mmol) and ascorbic acid (10 mg) were mixed in MeOH (40 mL), and the solution was stirred for 10 min to result in a yellow solution and a white precipitate. The solution was filtered, and the filtrate was added under Ar to a methanol (160 mL) solution of **1** (668 mg, 3.88 mmol). The mixture was then heated to reflux under Ar for 90 min. After cooling to room temperature, a yellow solid formed, which was recovered by filtration, washed and dried in air. Yield: 210 mg, 16% (based on Fe). The filtrate was left under a weak flow of Ar to allow slow evaporation of the solvent, which resulted in the formation of yellow crystals after about 24–36 h. These crystals, suitable for single-crystal X-ray analysis, contained variable amounts of lattice methanol, i.e., **2**·3.5MeOH or **2**·5MeOH. Indeed, they very rapidly lose crystallinity when exposed to air, probably loosing methanol and absorbing moisture from air, as indicated by elemental analysis of crystalline material dried in air. The crystals were kept under Ar in a small amount of mother solution or methanol. Prolonged storage (> 6 months) results in damage and partial oxidation of the crystals. $C_{49}H_{50}Fe_2N_{24}O_5S_4$ (**2**·5H_2O): calcd. C 45.44, H 3.89, N 25.96; found C 45.4, H 3.8, N 26.1. IR: $\tilde{\nu}$ = 3437 (br.), 3143, 3100, 3030, 2925, 2063, 1618, 1602, 1576, 1525, 1516, 1492, 1450, 1311, 1292, 1227, 1170, 1059, 1025, 955, 764, 752, 689, 623, 591, 501 cm^{-1}. The IR spectra of the crude yellow solid and the crystals were virtually identical. Overall yield (crystals and powder): 545 mg, 42%.

$[Co_2(\mathbf{1})_5(NCS)_4]$ (3): $CoSO_4\cdot 7H_2O$ (283 mg, 1.01 mmol) was dissolved in methanol (10 mL), and NH_4NCS (162 mg, 2.13 mmol) was added. The resulting mixture was stirred for 5 min and filtered. The filtrate was added to a methanol (100 mL) solution of **1** (430 mg, 2.50 mmol) to result in a clear pinkish solution, which was stirred at room temperature overnight. The fleshy solid formed was recovered by filtration, washed with MeOH and diethyl ether and dried in air. Yield: 230 mg, 18% (based on Co). $C_{49}H_{50}Co_2N_{24}O_5S_4$ (**3**·5H_2O): calcd. C 45.23, H 3.87, N 25.83; found C 45.0, H 4.0, N 25.5. IR: $\tilde{\nu}$ = 3426 (br.), 3151, 3100, 3030, 2971, 2067, 1618, 1602, 1575, 1527, 1515, 1490, 1448, 1310, 1292, 1227, 1171, 1059, 1026, 954, 763, 752, 685, 622, 592, 502 cm^{-1}. Single-crystals suitable for X-ray diffraction studies were obtained by slow concentration of the filtrate and were stored in their mother liquor or MeOH owing to loss of crystallinity upon air exposure. The IR spectra of the powder and crystals were virtually identical. Overall yield (crystals and powder): 630 mg, 48%.

$[Ni_2(\mathbf{1})_5(NCS)_4]$ (4): $NiSO_4\cdot 5H_2O$ (287 mg, 1.02 mmol) was dissolved in methanol (20 mL), and NH_4NCS (165 mg, 2.17 mmol) was added. The resulting mixture was stirred for 10 min and filtered. The filtrate was added to a methanol (90 mL) solution of **1** (427 mg, 2.48 mmol) to result in a clear blue solution, which was stirred at room temperature overnight. The fine purple solid formed was recovered by filtration, washed with MeOH and diethyl ether and dried in air. Yield: 655 mg, 50.3% (based on Ni). Attempts to grow single crystals from the filtrate were unsuccessful. $C_{49}H_{50}Ni_2N_{24}O_5S_4$ (**4**·5H_2O): calcd. C 45.24, H 3.87, N 25.84; found C 44.8, H 3.4, N 26.1. IR: $\tilde{\nu}$ = 3434 (br.), 3152, 3108, 3030, 2080, 1614, 1603, 1575, 1527, 1522, 1491, 1450, 1334, 1312, 1294, 1228, 1174, 1060, 998, 860, 762, 753, 690, 624, 592, 512 cm^{-1}.

$[Cu_2(\mathbf{1})_5(NCS)_4]$ (5): $CuSO_4\cdot 5H_2O$ (255 mg, 1.02 mmol) was dissolved in methanol (10 mL), and NH_4NCS (164 mg, 2.15 mmol) was added. The resulting reaction mixture was stirred for 5 min and filtered. The filtrate was added to a methanol (100 mL) solution of **1** (430 mg, 2.50 mmol) to result in a clear green solution, which was stirred at room temperature overnight. The green solid formed was recovered by filtration, washed with MeOH and diethyl ether and dried in air. Yield: 680 mg, 53% (based on Cu). Attempts to grow single crystals from the filtrate only resulted in the formation of very low quantities of tiny single crystals, which did not diffract sufficiently. $C_{49}H_{44}Cu_2N_{24}O_3S_4$ (**5**·3H_2O): calcd. C 46.18, H 3.64,

N 26.38; found C 45.8, H 3.3, N 26.8. IR: $\tilde{\nu}$ = 3153, 3113, 3094, 2978, 2122, 2109, 1612, 1601, 1576, 1519, 1515, 1494, 1476, 1453, 1311, 1290, 1226, 1173, 1053, 1028, 967, 882, 818, 773, 760, 749, 700, 692, 685, 624, 592, 510, 492, 464 cm^{-1}.

Structure Determination: Owing to the sensitivity of crystals of **2** and **3**, single-crystal diffraction experiments were performed by mounting crystals directly onto the goniometer with a cold N_2 stream by using the oil-drop method to reduce the loss of lattice solvent and the ensuing deterioration of crystallinity as much as possible. Data for compounds **2**·3.5MeOH at 100 and 250 K and **3**·3.5MeOH at 100 K were collected with a Bruker APEX II CCD diffractometer at the Advanced Light Source beamline 11.3.1 at Lawrence Berkeley National Laboratory from a silicon 111 monochromator (λ = 0.7749 Å). Data reduction and absorption corrections were performed with SAINT and SADABS,[31] respectively. Data for compound **2**·5MeOH at 150 and **2** at 296 K were obtained with an Oxford Diffraction Excalibur diffractometer with enhanced Mo-K_α radiation (λ = 0.71073 Å) at the X-ray diffraction and Fluorescence Analysis Service of the University of Zaragoza. Cell refinement, data reduction and absorption corrections were performed with the CrysAlisPro suite.[32] All structures were solved with SIR92[33] and refined on F^2 with the SHELXTL suite.[34] Crystal data collection and refinement parameters are given in Table S1. CCDC-901398 (for **2**·3.5MeOH, 100 K), -901399 (for **2**·3.5MeOH, 250 K), -901400 (for **2**·5MeOH, 150 K), -901401 (for **2**, 296 K) and -901402 (for **3**·3.5MeOH, 100 K) contain the supplementary crystallographic data for this paper. These data can be obtained free of charge from The Cambridge Crystallographic Data Centre via www.ccdc.cam.ac.uk/data_request/cif.

Supporting Information (see footnote on the first page of this article): Crystallographic data for **2**·3.5MeOH at 100 and 250 K, **2**·5MeOH at 150 K, **2** at 296 K and **3**·3.5MeOH at 100 K (Table S1), relevant structural parameters of the dinuclear complex and intermolecular interactions (Tables S2–S7). IR spectra of **2**–**5** (Figure S1), views of the crystal packing of **2**·3.5MeOH (Figures S2–S4), view of the crystal packing of **2** (Figure S5), view of the dinuclear complex in the structure of **3**·3.5MeOH (Figure S6).

Acknowledgments

P. G. acknowledges the Institució Catalana de Recerca i Estudis Avançats (ICREA). P. G. and O. R. are grateful to the Spanish Ministerio de Economía y Competitividad (MINECO) for funding (Projects CTQ2011-27929-C02-01 and MAT2011-24284). The Advanced Light Source is supported by the Director, Office of Science, Office of Basic Energy Sciences of the U. S. Department of Energy under contract no. DE-AC02-05CH11231.

[1] a) J. A. Real, A. B. Gaspar, M. C. Muñoz, *Dalton Trans.* **2005**, 2062–2079; b) P. Gamez, J. S. Costa, M. Quesada, G. Aromí, *Dalton Trans.* **2009**, 7845–7853; c) for a complete overview on spin-crossover systems, see: "Spin Crossover in Transition Metal Compounds I, II and III", P. Gütlich, H. A. Goodwin, *Top. Curr. Chem.* **2004**, *233*, *234* and *235*.

[2] P. Gütlich, A. Hauser, H. Spiering, *Angew. Chem.* **1994**, *106*, 2109; *Angew. Chem. Int. Ed. Engl.* **1994**, *33*, 2024–2054.

[3] P. Gütlich, Y. Garcia, H. A. Goodwin, *Chem. Soc. Rev.* **2000**, *29*, 419–427.

[4] a) G. Aromí, L. A. Barrios, O. Roubeau, P. Gamez, *Coord. Chem. Rev.* **2011**, *255*, 485–546; b) J. G. Haasnoot, *Coord. Chem. Rev.* **2000**, *200–202*, 131–185; c) Y. Garcia, V. Niel, M. C. Muñoz, J. A. Real, *Top. Curr. Chem.* **2004**, *233*, 229–257; d) P. J. van Koningsbruggen, *Top. Curr. Chem.* **2004**, *233*, 123–149.

[5] a) For a minireview, see: O. Roubeau, *Chem. Eur. J.* **2012**, *18*, 15230–15244; b) M. M. Dîrtu, C. Neuhausen, A. D. Naik, A. Rotaru, L. Spinu, Y. Garcia, *Inorg. Chem.* **2010**, *49*, 5723–5736 and references cited therein; c) O. Roubeau, M. Castro, R. Burriel, J. G. Haasnoot, J. Reedijk, *J. Phys. Chem. B* **2011**, *115*, 3003–3012 and references cited therein.

[6] A. Bousseksou, G. Molnár, L. Salmon, W. Nicolazzi, *Chem. Soc. Rev.* **2011**, *40*, 3313–3335.

[7] a) O. Kahn, J. Kröber, C. Jay, *Adv. Mater.* **1992**, *4*, 718–728; b) O. Kahn, E. Codjovi, *Phil. Trans. R. Soc. London A* **1996**, *354*, 359–379; c) O. Kahn, C. J. Martinez, *Science* **1998**, *279*, 44–48.

[8] a) J-F. Létard, P. Guionneau, N. Daro, *Nanoparticles of a spin transition compound*, WO 2007/065996, **2007**; b) T. Forestier, S. Mornet, N. Daro, T. Nishihara, S.-I. Mouri, K. Tanaka, O. Fouché, E. Freysz, J.-F. Létard, *Chem. Commun.* **2008**, 4327–4329; E. Coronado, J. R. Galán-Mascarós, M. Monrabal-Capilla, J. García-Martínez, P. Pardo-Ibáñez, *Adv. Mater.* **2007**, *19*, 1359–1361.

[9] a) O. Roubeau, A. Colin, V. Schmitt, R. Clérac, *Angew. Chem.* **2004**, *116*, 3345; *Angew. Chem. Int. Ed.* **2004**, *43*, 3283–3286; b) T. Fujigaya, D.-L. Jiang, T. Aida, *Chem. Asian J.* **2007**, *2*, 106–113; c) M. Rubio, D. López, *Eur. Polym. J.* **2009**, *45*, 3339–3346; d) P. Grondin, O. Roubeau, M. Castro, H. Saadaoui, A. Colin, R. Clérac, *Langmuir* **2010**, *26*, 5184–5195.

[10] a) O. Roubeau, B. Agricole, R. Clérac, S. Ravaine, *J. Phys. Chem. B* **2004**, *108*, 15110–15116; b) O. Roubeau, E. Natividad, B. Agricole, S. Ravaine, *Langmuir* **2007**, *23*, 3110–3117; c) C. Thibault, G. Molnár, L. Salmon, A. Bousseksou, C. Vieu, *Langmuir* **2010**, *26*, 1557–1560.

[11] a) T. Fujigaya, D.-L. Jiang, T. Aida, *J. Am. Chem. Soc.* **2005**, *127*, 5484–5489; b) P. Sonar, C. M. Grunert, Y.-L. Wie, J. Kusz, P. Gütlich, A. D. Schlüter, *Eur. J. Inorg. Chem.* **2008**, 1613–1622; c) Y.-L. Wie, P. Sonar, M. Grunert, J. Kusz, A. D. Schlüter, P. Gütlich, *Eur. J. Inorg. Chem.* **2010**, 3930–3941.

[12] R. N. Muller, L. van der Elst, S. Laurent, *J. Am. Chem. Soc.* **2003**, *125*, 8405–8407.

[13] a) P. Grondin, D. Siretanu, O. Roubeau, M.-F. Achard, R. Clérac, *Inorg. Chem.* **2012**, *51*, 5417–5426; b) A. B. Gaspar, M. Seredyuk, P. Gütlich, *Coord. Chem. Rev.* **2009**, *253*, 2399–2413.

[14] F. Prins, M. Monrabal-Capilla, E. A. Osorio, E. Coronado, H. S. J. van der Zant, *Adv. Mater.* **2011**, *23*, 1545–1549.

[15] G. Félix, K. Abdul-Kader, T. Mahfoud, I. A. Gural'skiy, W. Nicolazzi, L. Salmon, G. Molnár, A. Bousseksou, *J. Am. Chem. Soc.* **2011**, *133*, 15342–15345.

[16] A. Grosjean, N. Daro, B. Kauffman, A. Kaiba, J.-F. Létard, P. Guionneau, *Chem. Commun.* **2011**, *47*, 12382–12384.

[17] a) V. P. Sinditskii, V. I. Sokol, A. E. Fogelzang, M. D. Dutov, V. V. Serushkin, M. A. Porai-Koshits, B. S. Svetlov, *Zh. Neorg. Khim.* **1987**, *32*, 1950; b) Y. Garcia, P. J. van Koningsbruggen, G. Bravic, P. Guionneau, D. Chasseau, G. Luca Cascarano, J. Moscovici, K. Lambert, A. Michalowicz, O. Kahn, *Inorg. Chem.* **1997**, *36*, 6357–6365; c) K. Drabent, Z. Ciunik, *Chem. Commun.* **2001**, 1254–1255; d) Y. Garcia, P. J. van Koningsbruggen, G. Bravic, D. Chasseau, O. Kahn, *Eur. J. Inorg. Chem.* **2003**, 356–362; e) M. M. Dîrtu, A. Rotaru, D. Gillard, J. Linares, E. Codjovi, B. Tinant, Y. Garcia, *Inorg. Chem.* **2009**, *48*, 7838–7852; f) M. M. Dîrtu, C. Neuhausen, A. D. Naik, A. Rotaru, L. Spinu, Y. Garcia, *Inorg. Chem.* **2010**, *49*, 5723–5736.

[18] a) G. Vos, R. A. Le Fêbre, R. A. G. de Graaff, J. G. Haasnoot, J. Reedijk, *J. Am. Chem. Soc.* **1983**, *105*, 1682; b) G. Vos, R. A. G. de Graaff, J. G. Haasnoot, A. M. van der Kraan, P. de Vaal, J. Reedijk, *Inorg. Chem.* **1984**, *23*, 2905–2910; c) M. Thomann, O. Kahn, J. Guilhem, F. Varret, *Inorg. Chem.* **1994**, *33*, 6029–6037; d) J. J. A. Kolnaar, G. van Dijk, H. Kooijman, A. K. Spek, V. G. Ksonofontov, P. Gütlich, J. G. Haasnoot, J. Reedijk, *Inorg. Chem.* **1997**, *36*, 2433–2440; e) Y. Garcia, P. Guionneau, G. Bravic, D. Chasseau, J. A. K. Howard, O. Kahn, V. Ksenofontov, S. Reiman, P. Gütlich, *Eur. J. Inorg. Chem.* **2000**, 1531–1538; f) M. B. Bushuev, L. G. Lavrenova, Y. G. Shvedenkov, A. V. Virovets, L. A. Sheludyakova, S. V. La-

rionov, *Russ. J. Inorg. Chem.* **2007**, *52*, 46–51; g) D. Savard, C. Cook, G. D. Enright, I. Korobkov, T. J. Burchell, M. Murugesu, *CrystEngComm* **2011**, *13*, 5190–5197; h) W. Vreugdenhil, J. G. Haasnoot, M. F. J. Schoondergang, J. Reedijk, *Inorg. Chim. Acta* **1987**, *130*, 235–242; i) L. R. Groeneveld, R. A. Le Fêbre, R. A. G. de Graaff, J. G. Haasnoot, G. Vos, J. Reedijk, *Inorg. Chim. Acta* **1985**, *102*, 69–82.

[19] a) A. Michalowicz, J. Moscovici, B. Ducourant, D. Cracco, O. Kahn, *Chem. Mater.* **1995**, *7*, 1833–1842; b) A. Michalowicz, J. Moscovici, O. Kahn, *J. Phys. IV* **1997**, *7*, 633; c) M. Verelst, L. Sommier, P. Lecante, A. Mosset, O. Kahn, *Chem. Mater.* **1998**, *10*, 980–985; d) T. Yokoyama, Y. Murakami, M. Kiguchi, T. Komatsu, N. Kojima, *Phys. Rev. B* **1998**, *58*, 14238–14244.

[20] a) D. W. Engelfriet, G. C. Verschoor, W. J. Vermin, *Acta Crystallogr., Sect. B* **1979**, *35*, 2927–2931; b) D. W. Engelfriet, G. C. Verschoor, W. den Brinker, *Acta Crystallogr., Sect. B* **1980**, *36*, 1554–1560; c) G. Vos, J. G. Haasnoot, G. C. Verschoor, J. Reedijk, *Inorg. Chim. Acta* **1985**, *102*, 187–198; d) J. J. A. Kolnaar, M. I. de Heer, H. Kooijman, A. L. Spek, G. Schmitt, V. Ksenofontov, P. Gütlich, J. G. Haasnoot, J. Reedijk, *Eur. J. Inorg. Chem.* **1999**, 881–886; e) H. S. Yoo, J. H. Lim, J. S. Kang, E. K. Koh, C. S. Hong, *Polyhedron* **2007**, *26*, 4383–4388; f) Y. Garcia, F. Robert, A. D. Naik, G. Zhou, B. Tinant, K. Robeyns, S. Michotte, L. Piraux, *J. Am. Chem. Soc.* **2011**, *133*, 15850–15853.

[21] a) With Ni^{II}: C. W. Reimann, M. Zocchi, *Acta Crystallogr., Sect. B* **1971**, *27*, 682–691; b) mixed-valent Co^{II}–Co^{III}: L. Antolini, A. C. Fabretti, D. Gatteschi, A. Giusti, R. Sessoli, *Inorg. Chem.* **1991**, *30*, 4860–4863; with Cu^{II}: J. Liu, Y. Song, Z. Yu, J. Zhuang, X. Huang, X. You, *Polyhedron* **1999**, *18*, 1491–1494; Y. Carcia, P. J. van Koningsbruggen, H. Kooijman, A. L. Spek, J. G. Haasnoot, O. Kahn, *Eur. J. Inorg. Chem.* **2000**, 307–314.

[22] J. G. Haasnoot, G. Vos, W. L. Groeneveld, *Z. Naturforsch. B* **1977**, *32*, 1421.

[23] P. Guionneau, M. Marchivie, G. Bravic, J.-F. Létard, D. Chasseau, *J. Mater. Chem.* **2002**, *12*, 2546–2551.

[24] P. Guionneau, M. Marchivie, G. Bravic, J.-F. Létard, D. Chasseau, *Top. Curr. Chem.* **2004**, *234*, 97–128.

[25] a) J. H. van Vleck, *The Theory of Electric and Magnetic Susceptibility*, Oxford University Press, Oxford, **1932**; b) K. Kambe, *J. Phys. Soc. Jpn.* **1950**, *5*, 48–51; c) for susceptibility expressions of pairs of *S* spins, see: C. J. O'Connor, *Prog. Inorg. Chem.* **1982**, *29*, 203.

[26] F. E. Mabbs, D. J. Machin, *Magnetism and Transition Metal Complexes*, Chapman and Hall Ltd., London, **1973**.

[27] a) A. Grosjean, P. Négrier, P. Bordet, C. Etrillard, D. Mondieig, S. Pechev, E. Lebraud, J.-F. Létard, P. Guionneau, *Eur. J. Inorg. Chem.* **2013**, 796–802; b) P. Guionneau, lecture at the MOLMAT2012 conference, Barcelona, July **2012**.

[28] a) J. Linarès, H. Spiering, F. Varret, *Eur. Phys. J. B* **1999**, *10*, 271–275; b) K. Boukheddaden, J. Linarès, H. Spiering, F. Varret, *Eur. Phys. J. B* **2000**, *15*, 317–326.

[29] K. Kuroiwa, T. Shibata, A. Takada, N. Nemoto, N. Kimizuka, *J. Am. Chem. Soc.* **2004**, *126*, 2016.

[30] G. A. Bain, J. F. Berry, *J. Chem. Educ.* **2008**, *85*, 532–536.

[31] *SAINT* and *SADABS*, Bruker AXS Inc., Madison, Wisconsin, USA.

[32] *CrysAlis PRO*, Agilent Technologies, Yarnton, UK.

[33] A. Altomare, M. C. Burla, G. Camalli, G. Cascarano, C. Giacovazzo, A. Gualiardi, G. Polidori, *J. Appl. Crystallogr.* **1994**, *27*, 435–436.

[34] G. M. Sheldrick, *Acta Crystallogr., Sect. A* **2008**, *64*, 112–122; G. M. Sheldrick, *SHELXTL*, Bruker AXS Inc., Madison, Wisconsin, USA.

Received: September 21, 2012
Published Online: November 26, 2012

